Odd-Even Quantisation and Cartesian Delta-Sigma (ΔΣ) Upconverters for Transmitter Design

Sirmayanti Sirmayanti[1,2], Vandana Bassoo[3], Horace King[1], Mike Faulkner[1]

[1]School of Engineering and Science, Victoria University, Melbourne, Australia
[2]Telecommunication Engineering Study Program, the State Polytechnic of Ujung Pandang, Indonesia
[3]School of Innovative Technologies and Engineering, University of Technology, Mauritius
E-mail: {sirmayanti.sirmayanti} @live.vu.edu.au

Abstract--This paper offers an alternative odd-quantisation approach scheme for Cartesian ΔΣ systems proposed for the all-digital upconversion of baseband modulation to radio frequency (RF). The developed Cartesian ΔΣ system with even-quantisation has a minimum pulsewidth of two clock periods. This leads to a potential coarse quantisation at low signal levels. We show that the noise problem can be reduced with a new odd-quantisation scheme which is based on pulses with an odd number of clock periods. In this paper, the minimum pulsewidth is reduced to one clock period. Other quantized amplitudes are obtained by incrementing the pulsewidth in steps of two clock periods, which maintains a constant phase reference. In both cases separate quantisers for amplitude and phase enable simple implementation. We show that both odd and even-quantisation schemes produce the same distortion products that increase with frequency offset. The odd-quantisation scheme, however, has improved SNR by approximately 2 dB.

I. INTRODUCTION

The demand for broadband wireless connectivity has forced the development of wireless standards with higher spectrum efficiency and wider bandwidth. As a consequence, signals suffer from high peak-to-average power ratios (e.g. Code Division Multiple Access (CDMA) and Orthogonal Frequency Division Multiplexing (OFDM)). Power amplifier (PA) linearity in the transmitter to be requiring critical [1,2]. The base-station (BS) also needs to operate with high energy efficiency. The combined requirements of high bandwidth, high efficiency, linearity and signal dynamics make the design of RF-PAs difficult.

Indoor wireless systems use low power Femtocell or WLAN networks. They often share frequencies with other users [3,4]. Consequently, this activity may cause interference to other users in surrounding networks [5-7]. Therefore, the indoor wireless systems require frequency flexibility to change channel quickly and avoid interference with other networks. In addition, they must have high efficiency and good linearity.

A promising approach towards high efficiency linear radio RF-PAs has been proposed [2]. All nonlinear PA classes can be operated with a switching input waveform, resulting in switch mode power amplification (SMPA). Pulse width and pulse position modulation (PWM/PPM) can be used to generate an RF signal with any amplitude and phase. Therefore, it is an important technique in switched mode transmitter architectures. This has led to renewed interest in transceiver architectures based on PWM/PPM for the upconversion to RF or intermediate frequency (IF) of baseband signals.

PWM/PPM signals are usually quantized in both amplitude and phase. The amplitude and phase of the RF signals are controlled by the pulse width and pulse position of the switched mode output respectively. Normally, baseband signals are generated in Cartesian format. Therefore, these signals must be converted to Polar format to generate PWM/PPM signals.

A novel all digital approach to generate a pulse train for driving an SMPA was proposed in [8]. The authors developed a Cartesian ΔΣ system to generate a binary signal with an appropriate pulse width and pulse position. ΔΣ techniques was used to shape the noise away from the band of interest. They operate by subtracting the current quantised error signal from the subsequent sample [9]. The Cartesian ΔΣ technique shown in Fig.1 was used to suppress the quantisation noise but the 'Polar to PWM/PPM' block can generate unwanted spectral components when the carrier frequency of the transmitted signal is offset from its nominal frequency [10,11]. The proposed quantiser in [10,11] used an even-quantisation technique where the three-level-waveform at the output is based on pulses with an even number of clock periods. The quantised amplitudes, $\hat{R}$, of the RF signal are calculated by changing the pulsewidths in increments of two clock periods. This leads to a potential coarse quantisation at low signal levels as the minimum pulsewidth in the even-quantization scheme is two clock periods.

It should be noted that most of today's modulation schemes have large signal dynamics. OFDM and CDMA are often modeled with a Rayleigh amplitude distribution. The signals must be backed off so that the electronics can handle the peak powers. The result is that there is an increased probability of low signal levels in the ΔΣ modulator. Ideally therefore the quantisation levels should also be concentrated at the low signal levels. This paper offers an alternative approach to the even-quantisation of [10].

Odd-quantisation is proposed to reduce the possible pulsewidths by one clock period while maintaining a constant phase reference. The acceptable pulsewidths become (0, 1, 3, 5 ...) for the odd-quantisation compared to the (0, 2, 4, 6 ...) values for the even-quantisation. In both cases the phase reference does not change with the pulsewidth, allowing separate quantisers for amplitude and phase. We show that the noise problem can be reduced using the odd-quantisation method.

The paper is organized as follows. Section II presents the Cartesian ΔΣ upconverters. Section III gives details of the new

odd-quantisation scheme. Section IV gives results of comparison between the even and odd-quantisation schemes. Finally, we draw a conclusion in section V.

II. CARTESIAN $\Delta\Sigma$ UPCONVERTERS

A $\Delta\Sigma$ modulator is used to fit the required resolution by reducing the quantisation noise which is a by-product of the discretisation process [9]. $\Delta\Sigma$ techniques have been proposed to shape the noise away from the carrier frequency in the band of interest [12-15]. This concept has contributed to the elimination of many analog components (such as high performance analog-to-digital and digital-to-analog converters (ADCs/DACs), the quadrature modulator and local oscillator) in current direct conversion wireless transmitters [16].

$\Delta\Sigma$ modulation is achieved through the processes of oversampling and noise shaping. Oversampling reduces the noise power spectral density (PSD) as it spreads the noise over a wider bandwidth. As expected, increasing oversampling rate (OSR) will decrease the in-band noise proportional to $\frac{1}{OSR}$ [9].The oversampling ratio of the baseband (BB) is given by

$$OSR_{BB} = \frac{f_S}{2f_B} \qquad (1)$$

where f_B is the maximum signal bandwidth and f_s is the sampling frequency. The quantisation error is also noise shaped using feedback in the $\Delta\Sigma$ filter. The noise transfer function (NTF) for a lowpass 2nd order $\Delta\Sigma$ is given by:
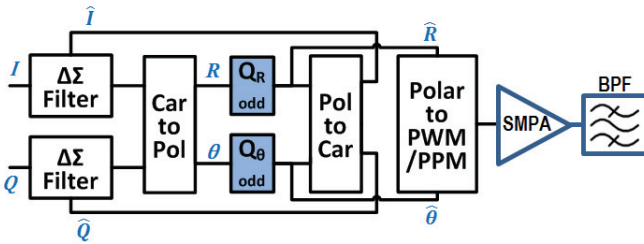
$$NTF = (1 - z^{-1})^2 \qquad (2)$$

Fig. 1. Cartesian $\Delta\Sigma$ Upconverters. Q_R and Q_θ quantise the amplitude and phase.

The Cartesian $\Delta\Sigma$ upconverters structure [11,12] can be seen in Fig. 1. It consists of two second-order (MOD2) lowpass $\Delta\Sigma$s [9] for the Cartesian I and Q input signals. After $\Delta\Sigma$ filtering, the I and Q signals are converted to Polar coordinates $[R, \theta]$ and separately quantised in the Q_R and Q_θ blocks. The output of the quantisers $[\hat{I}, \hat{Q}]$ are converted back to Cartesian coordinates (removing bandwidth expansion) and fed back to the $\Delta\Sigma$ filters. The outputs of both quantisers $[\hat{R}, \theta]$ are also upconverted to RF using PWM/PPM techniques in the 'Polar to PWM/PPM' block.

III. NEW QUANTISATION SCHEME
A. Q_R and Q_θ block with odd-quantisation
The PWM/PPM process requires the digital clock (f_{clock}) to oversample the nominal RF carrier frequency of the signal output (f_c) by a factor of OSR_{RF}. The OSR_{RF} is given by

$$OSR_{RF} = \frac{f_{clock}}{f_c} \qquad (3)$$

The phase is therefore uniformly quantised into a number of phase quantised levels of N_P ($=OSR_{RF}$) increments over the range 0 to 2π. The quantised phase, $\hat{\theta}$, is determined by the

pulse position. The quantised amplitude, $\hat{R}$, is determined by the pulse width as shown in Fig. 2. The top trace shows the maximum amplitude condition for OSR_{RF}=8. The output is a full square wave, and after bandpass filtering produces the sinusoidal output. The second trace down shows a reduced amplitude sinewave caused by the reduced pulse widths of the three-level waveform. The third trace shows the zero amplitude sinewave. The $\Delta\Sigma$ filter cycles the output between these three quantised states to generate any specified amplitude of the RF signal.
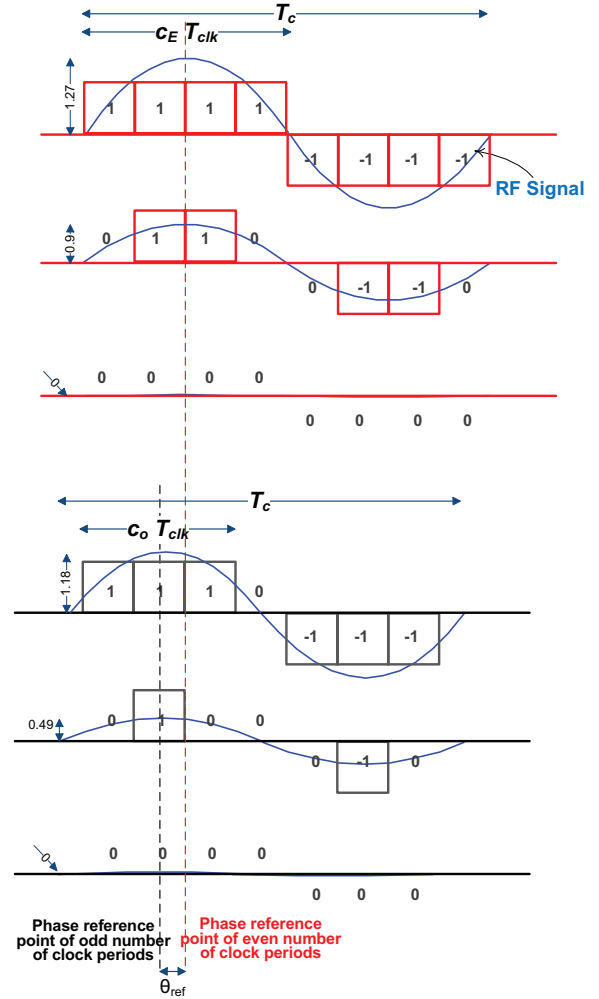

Fig. 2. Comparison of calculation for quantisation amplitude with the even-odd number of clock periods, OSR_{RF}=8.

The top three traces show pulse widths that contain an even number of clock periods, and the bottom three traces show the odd sized pulse widths. The phase reference is taken from the middle of the pulse and is 0 degrees for even pulse widths. However the reference for odd pulse widths is given by

$$\theta_{ref} = \frac{2\pi/N_P}{2} \qquad (4)$$

If the quantised amplitudes, $\hat{R}$, are confined to all the even pulse widths, then the phase reference does not change and so amplitude quantisation and phase quantisation are independent one dimensional operations; similarly, if the quantisation amplitudes are confined to all the odd pulsewidths. When both odd and even pulse widths are allowed a change in amplitude

can cause a change in phase (AM to PM conversion) and so joint amplitude and phase quantisation must be applied. This is a two-dimensional operation and leads to a great increase in quantiser complexity.

Fig. 3 shows the odd-even quantisation in the polar plane. The radius of the circles is set by $\hat{R}$. The radial lines show the quantised phase, $\hat{\theta}$. The even-quantised points of $Q_E[\hat{R},\hat{\theta}]$ are illustrated by red dots (intersection between the red thick lines and red circles). The odd-quantised points of $Q_O[\hat{R},\hat{\theta}]$ are illustrated by the black crosses (intersection between the black thin lines and black circles). $\hat{R}$ and $\hat{\theta}$ are the quantised values of $[R,\theta]$ corresponding to the I and Q output of the $\Delta\Sigma$ filters. The dashed circles between each of three circles (red is for even-polar, and black is for odd-polar) are the threshold levels for the amplitude quantiser (L_R). The number of threshold levels for the amplitude, n_{L_R}, is given by

$$n_{L_R} = N_A - 1 \qquad (5)$$

where N_A is number of level amplitude increments. N_A is determined by OSR_{RF}.

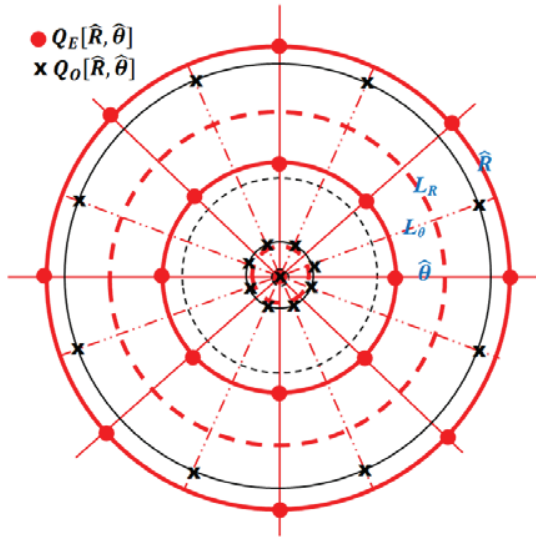$$N_A = \left(\frac{OSR_{RF}}{4} + 1\right) \qquad (6)$$

Fig. 3. The odd-even quantisation polar plane scale, $OSR_{RF}=8$.

The phase threshold levels, (L_θ), are measured midway between two phase increments, and are shown dashed for the even-quantisation. The number of phase threshold levels, n_{L_θ}, is the same as the number of phase quantised levels, given by

$$n_{L_\theta} = N_P \qquad (7)$$

The proposed even-quantisation technique leads to a potential coarse quantisation at low signal levels, as shown by the inner (red) circle in Fig. 3. Therefore, we propose the odd-quantisation scheme to refine the quantisation at low signal levels by changing the minimum pulsewidth to one clock period while maintaining constant phase reference. The first quantisation level is now smaller (pulse width of 1). The largest quantisation level is also reduced but by a smaller amount. A calculation of the quantisation amplitude and phase levels which correspond to pulse widths with an odd number of clock periods is now shown.

TABLE I
VALUES OF $\hat{R}_Q$ FOR DIFFERENT OSR

p_o	OSR (=N_P)					Q
p_E	4	6	16	32	64	
0	0	0	0	0	0	
1	0.9003	0.4873	0.2484	0.1248	0.0625	
3	-	1.1763	0.7074	0.3696	0.1868	
5	-	-	1.0587	0.6002	0.3094	
7	-	-	1.2488	0.8078	0.4290	
9	-	-	-	0.9843	0.5444	
11	-	-	-	1.1229	0.6546	O
13	-	-	-	1.2184	0.7585	
15	-	-	-	1.2671	0.8551	D
17	-	-	-	-	0.9434	
19	-	-	-	-	1.0227	D
21	-	-	-	-	1.0921	
23	-	-	-	-	1.1510	
25	-	-	-	-	1.1988	
27	-	-	-	-	1.2351	
29	-	-	-	-	1.2595	
31	-	-	-	-	1.2717	
0	0	0	0	0	0	
2	1.2733	0.9003	0.4873	0.2484	0.1248	
4	-	1.2733	0.9003	0.4873	0.2484	
6	-	-	1.1763	0.7074	0.3696	
8	-	-	1.2733	0.9003	0.4873	E
10	-	-	-	1.0587	0.6002	
12	-	-	-	1.1763	0.7074	V
14	-	-	-	1.2488	0.8078	
16	-	-	-	1.2733	0.9003	E
18	-	-	-	-	0.9843	
20	-	-	-	-	1.0587	N
22	-	-	-	-	1.1229	
24	-	-	-	-	1.1763	
26	-	-	-	-	1.2184	
28	-	-	-	-	1.2488	
30	-	-	-	-	1.2671	
32	-	-	-	-	1.2733	

The amplitude levels are calculated by evaluating the fundamental spectral component of the three-level waveform, $u_n(p_o, p_p)$, with amplitudes 1, 0, and -1. p_o is the pulsewidth corresponding to the c_O clock cycles (c_O is for odd) or c_E clock cycles (c_E is for even). p_p is the pulse position and refers to the time delay or advance. $p_p = (0, \dots (N_P-1))$ and represents the PPM delay in clock periods.

Since $u_n(p_o, p_p)$ is a repeating waveform, the amplitude of the spectral component can be generated from one period only using the Fourier series. Here, we use a highly oversampled version of $u_n(p_o, p_p)$ to get the same result from a discrete Fourier transform (DFT).

$$U_k(p_o, p_p) = \frac{1}{K} DFT(u_n(p_o, p_p)) \qquad (8)$$

where K is the fast Fourier transform (FFT) size. The amplitude of the fundamental of the pulse wave occurs in the first frequency bin, $k=1$

$$\hat{R}_Q\left(\frac{p_o}{2}\right) = 2\big[|U_{k=1}(p_o, p_p)|\big], \qquad (9)$$

$\left(\frac{p_o}{2}\right)$ is the index for the different pulsewidths corresponding to the odd pulsewidth $\left(0, \frac{1}{OSR_{RF}}, \frac{3}{OSR_{RF}} \dots \frac{N_P-1}{OSR_{RF}}\right)\frac{1}{f_c}$.

The amplitude threshold levels are given by the midpoint of two amplitude quantised levels,

$$L_R\left(\frac{p_o}{2}, \frac{p_o}{2}+1\right) = \frac{R\left(\frac{p_o}{2}\right)+R\left(\frac{p_o}{2}+1\right)}{2}, \qquad (10)$$

where the index of $\frac{p_o}{2}$ is selected in ascending order.

The quantised phase is based on the odd-polar plane, as shown in Fig. 3. The quantised phase is given by

$$\hat{\theta}_Q = (p_p + 0.5)\frac{2\pi}{N_P} \quad (11)$$

The threshold for the quantised phase is calculated by equation

$$L_\theta(p_p, p_p + 1) = p_p\frac{2\pi}{N_P} \quad (12)$$

Table I shows the pulsewidth (normalised) and the quantised amplitudes of the resulting RF signals for even and odd schemes. The number of quantised amplitudes, N_A, is determined by (6). There are OSR clock periods in one cycle of f_c and OSR_{RF} is equal to N_P.

Fig. 4 illustrates the quantisation steps of $\hat{R}_Q$ on Q_R for the odd and even schemes. As it is shown, the example is taken based on Table I when N_P=16.
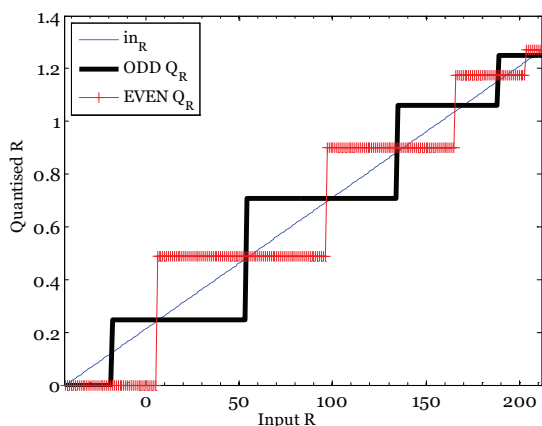

Fig. 4. Quantisation steps of $\hat{R}_Q$ on Q_R, Np=16.

B. 'Polar to PWM/PPM' Block

This block is used to convert the quantised signals, $[\hat{R}, \hat{\theta}]$, in Polar representation to RF using PWM and PPM schemes. The location of the pulse position of the PPM process is determined using the quantised phase, $\hat{\theta}$, which is the output from Q_θ block. A change in position depends on a change of $\hat{\theta}$ where the pulse edges must occur on the digital timing grid. The output of Q_R block, $\hat{R}$, determines the duration of the PWM process.
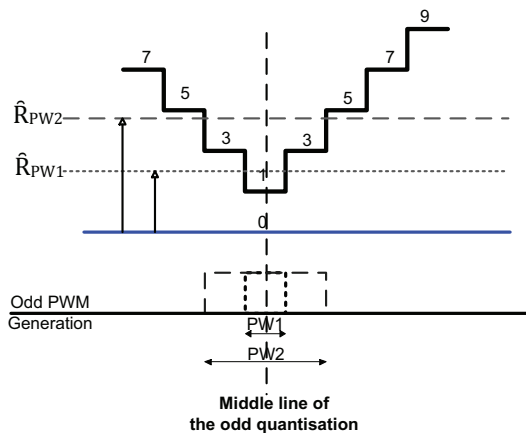

Fig. 5. Odd PWM generation using a stepped triangular reference signal.

Fig. 5 illustrates the PWM generation of odd quantised signals using a stepped triangle wave. It shows two examples of quantised amplitudes: $\hat{R}_{PW1}$ and $\hat{R}_{PW2}$. The output pulsewidths, PW1 and PW2, are defined by the crossing points of the line $\hat{R}_{PW1}$ and $\hat{R}_{PW2}$ respectively and the stepped triangular waveform signal. The pulsewidth must change with two sample increments to decouple the amplitude response from the phase response. The pulsewidth then maintains symmetry about its midpoint.

IV. SIMULATION RESULTS

In this section the performance of the odd-quantisation scheme is measured. Here, the carrier frequency f_c is normalised to 1.024 GHz, and OSR_{RF}=32. The test signal is a single side band (SSB) tone.
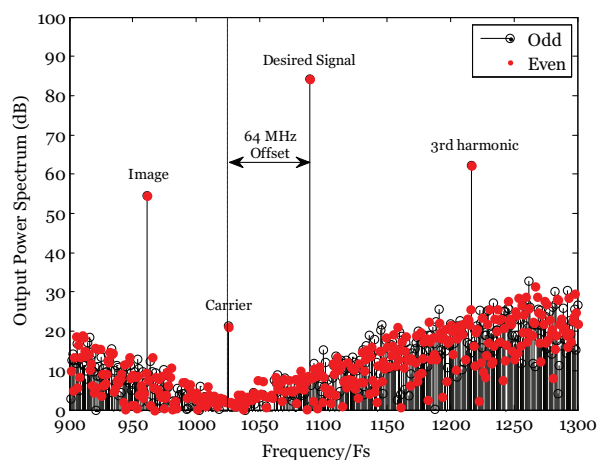

Fig. 6. Output Spectrum of 'Polar to PWM/PPM' block.

Fig. 6 shows the frequency spectrum of a SSB signal which is offset by 64 MHz from the carrier. The results are given at the output of the 'Polar to PWM/PWM' block. The spectrums of both the even and the odd quantisation are drawn for comparison purpose. The black dots show the even-quantisation while the hollow circles show the odd-quantisation.

Offsetting the carrier frequency from the nominal centre frequency (f_c) causes distortion products to occur. As shown on Fig. 6, the dominant distortion products are the image and odd order harmonics (1st harmonic and 3rd harmonic). The signal itself is the 1st harmonic. The image and 3rd are unwanted signals. The noise is nulled at the nominal carrier frequency by the $\Delta\Sigma$ operation. The further the signal is from this point the greater is its accompanying noise (leading to larger in band error vector magnitude (EVM)).

The amplitudes of each distortion product were compared for the even and the odd quantisation schemes. As shown in Fig. 7, the size of unwanted distortion products in the odd-quantisation scheme reduces slightly compared to the even-quantisation scheme. The 3rd harmonic is the largest distortion component. As shown in Table II, the amplitudes of the signals and the signal-to-noise ratio (SNR) of the desired signals between both schemes are compared. The noise power was calculated for different offset frequencies and a signal bandwidth of 16 MHz (or fc/64).
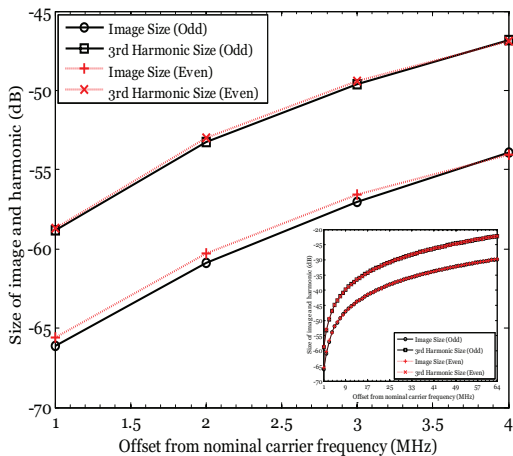
Fig. 7. Zoom In of sizes of the unwanted signals against 64 MHz of offset frequency (f_c=1024 GHz), dB relative to carrier.

TABLE II
COMPARISON OF THE ODD-EVEN SCHEMES ON THE SNR AT THE SIGNAL

| Offset carrier frequency | SNR, dB | |
	Odd-quantisation scheme	Even-quantisation scheme
16	92.5	89.4
32	87.8	85.4
64	80.4	78.9
128	70.7	69.8
256	59.0	58.4

The signal amplitudes remain stable for all carrier frequency offsets. Interestingly, the signal amplitude for the odd-quantisation scheme was slightly reduced compared to the even-quantisation scheme. As expected SNR's degrade as the signal is moved into noisier parts of the spectrum as the frequency offsets increase. More interestingly, the odd-quantisation scheme has an average improved SNR of about 2 dB compared to the even-quantisation scheme. This was anticipated for OFDM like signals where low signal magnitudes dominate, but seems to also apply to continuous wave (CW) SSB signals. The explanation is due to the noise components that are part of the $\Delta\Sigma$ output waveform. Even greater improvement is expected for OFDM modulation.

The effect of odd-even quantisation on the image and odd order distortion products is less pronounced. These distortions are caused by the phase quantisation [11] and will make it hard for either scheme to work with a large frequency offset.

V. CONCLUSION

An analysis of the noise and distortion products of the odd-quantisation compared to the even-quantisation schemes has been investigated. The dominant distortions are arising in the 'Polar to PWM/PPM' block in these schemes. Both the odd and even-quantisation schemes produce the same distortion products. The power of the unwanted distortion products is only marginally reduced in the odd-quantisation scheme. The simulation results showed that the size of all distortion products with respect to the signal increased with increasing

offset frequency for a SSB signal. Signal offsetting is therefore not recommended for channel tuning, rather the clock frequency should be altered for frequency agility. The main benefit of the odd-quantisation scheme is the SNR improvement of about 2 dB. Therefore, the odd-quantisation scheme is preferred over the even-quantisation scheme.

VI. ACKNOWLEDGEMENT

VII. REFERENCES

[1] P. Lavrador, T. Cunha, P. Cabral, and J. Pedro, "The linearity-efficiency compromise", IEEE Microw. Mag., vol.11, no. 5, pp. 44-48, Aug 2010.
[2] H. Sjoland, et al, "Switched Mode Transmitter Architectures," in Analog Circuit Design Smart Data Converters, Filters on Chip, Multimode Transmitters, A.H.M Van Roermund, Ed. Netherlands: Springer, pp. 325-342, 2009.
[3] W. Yi, Z. et.al. "A Novel Spectrum Arrangement Scheme For Femtocell Deployment In LTE Macrocells" in Proc. IEEE 20th Int. Symp PIMRC Japan, Sep 2009.
[4] P. Pirinen, "Co-Channel Co-Existence Study Macrocell and Indoor Femtocell Users" in Proc. European Wireless Conference (EW'10) Italy, pp. 207–213, Apr 2010.
[5] D. Lopez-Perez, et.al, "OFDMA Femtocells: A Roadmap on Interference Avoidance", IEEE Communications Magazine, Vol. 47, Issue 9, pp. 41–48, Sep 2009.
[6] Y.Tokgoz, et.al, "Uplink Interference Management for HSPA+ and 1xevdo Femtocells" in Proc. IEEE, GLOBECOM, Honolulu, Dec 2009.
[7] S. Zhenning, R. Mark C., and Z.Ming, "On Uplink Interference Scenarios in Two-Tier Macro and Femto Co-Existing UMTS Networks", EURASIP journal on Wireless Comm. & Networking, Vol 2010.
[8] V. Bassoo and M. Faulkner, "Sigma Delta Digital Drive Signals for Switch mode Power Amplifiers", Electronic Letters, Vol. 44, Issue 22, pp. 1299-1300, Oct 2008.
[9] R. Schreier and G.C. Temes, "Understanding delta-sigma data converters", Wiley Press, 2004.
[10] V. Bassoo, A. Mustafa, M. Faulkner, "Distortion arising from polar to PWM/PPM conversion in an all digital up converter for switching RF power amplifier". In Proc. IEEE IMS Int. Microwave Symp., Boston, USA, pp. 1533–1536, Jun 2009.
[11] V. Bassoo, Linton L., Faulkner M., "Analysis of distortion in pulse modulation converters for switching radio frequency power amplifiers", IET Microwave Antennas Prop. Vol. 4, Issue. 12, pp. 2088-2096, Dec 2010.
[12] S. Sirmayanti, H. King, V. Bassoo, and M. Faulkner "Sigma Delta ($\Sigma\Delta$) Architecture Integration with Digital Pre-distortion to enhance Optimal Switch Mode Power Amplification (OSMPA) in FEMTO cell Transceiver Design", in Proc. IEEE 8th ICICS, Singapore, Dec 2011.
[13] V. Bassoo et.al, "A potential transmitter architecture for future generation green wireless base station", EURASIP Journal on Wireless Com. & Net. Article ID 821846, 8 pages, 2009.
[14] U. Gustavsson, T. Eriksson, and C. Fager, "Quantisation noise minimization in $\Sigma\Delta$ modulation based RF transmitter architectures", IEEE Trans. Circuits Syst.I, vol. 57, no. 12, pp. 3082-3091, Dec 2010.
[15] B. T. Thiel and R. Negra, "Quad-phase lowpass delta-sigma modulator for switching-mode power amplifier", in Proc. IEEEAsia Pacific Microwave Conference (APMC 2011), pp. 131-134, Dec 2011.
[16] B. Razavi, "RF microelectronics", Prentice Hall Ptr, 1998.
[17] V. K. Ingle and J. G. Proakis, " Digital Signal Processing using Matlab", Bill Stenquist, 2000.